

High-Frequency Geoacoustic Inversion of Ambient Noise Data Using Short Arrays

Martin Siderius* and Chris Harrison †

*Center for Ocean Research, SAIC, 10260 Campus Point Drive, San Diego, CA, 92121

†NATO Undersea Research Centre 400 Viale San Bartolomeo, La Spezia Italy, 19138

Abstract. Ocean ambient noise is generated in many ways such as from winds, rain and shipping. A technique has recently been developed (Harrison and Simons, *J. Acoust. Soc. Am.*, Vol. 112 no. 4, 2002) that uses the vertical directionality of ambient noise to determine seabed properties. It was shown that taking a ratio of upward looking beams to downward produces an estimate of the reflection loss. This technique was applied to data in the 200–1500 Hz band using a 16-m vertical array. Extending this to higher frequencies allows the array length to be substantially shortened and greatly reduces interference from shipping. If array lengths can be reduced to about 1 m then it may be possible to hull-mount or tow such an array from a surface ship or submerged vehicle (e.g. an autonomous underwater vehicle). Although this seems attractive the noise is primarily generated by wind which in turn causes a rough sea-surface and bubbles and these factors combined with increased volume attenuation may degrade this type of reflection loss estimate at high frequencies. In this paper, we examine measured noise data from the October 2003 ElbaEx experiment using a 5.5 m array in the 1–4 kHz frequency band. Results indicate the noise field is predictable with modeling and the ratio of upward looking to downward looking beams produces an approximation to the reflection loss which can be inverted for seabed properties. For short arrays (a 1 m aperture is considered here), the beamforming is not ideal over a broad-band of frequencies. The beams are broadened and this leads to an up/down ratio that does not produce a good estimate of reflection loss. This can be especially problematic at low grazing angles which is the part of the reflection loss curve that is often most important to estimate correctly. Techniques will be presented for mitigating the impact of beamwidth and grating lobes on estimating the seabed properties.

INTRODUCTION

Using measurements of ocean ambient noise to produce an estimate of seabed properties is attractive for several reasons. 1) Since ambient noise results from wind and rain interacting with the sea-surface the sound sources exist everywhere. 2) This sheet source provides an angular spread of plane-waves that have interacted with the bottom and therefore contain information about seabed properties. 3) Passive measurements not requiring a sound projector greatly simplify the design of an experiment or survey technique. 4) With concerns over the impact of sound on marine mammals, an environmentally friendly geoacoustic inversion method that does not require a human-made sound source is highly attractive.

Although the dependency of ambient noise on seabed properties has been widely reported, only recently has a method been developed that uses vertical directionality of ambient noise data to produce the bottom power reflection loss. This was demonstrated for several sites using a 16 m vertical aperture for frequencies of 200–1500 Hz [1].

The method uses a ratio between beams traveling from the direction of the surface to those coming from the seabed and in theory this ratio equals the bottom power reflection loss. Actual beamforming introduces beam widths and this can be a big problem as array lengths become short (relative to wavelength) or when hydrophone spacing is larger than half a wavelength and grating lobes are introduced that erroneously mix the up and down going beams. Beamforming and separating up and downgoing beams can be especially problematic near grazing angles which is important for longer range propagation.

For practical applications, it is difficult to cover large areas using long vertical arrays. It is possible to have long vertical arrays drift to determine bottom properties and even a sub-bottom profile [2]. However, it is difficult to tow them in a specific pattern such as during a multibeam bathymetry survey. For this, short arrays are attractive since these can be towed or mounted on the hull of a surface ship, or these could be mounted on an autonomous underwater vehicle (AUV). If short vertical apertures are feasible it may even be possible to use the slight tilt in long towed arrays. As vertical aperture shrinks, it is natural to shift to higher frequencies and this has the added benefit of operating outside the frequency band dominated by shipping. While distant shipping noise does not generally cause a major concern, nearby shipping can interfere with the beamformed output in such a way that the reflection loss estimates are not valid.

In this paper we examine using high-frequency (1–4 kHz) noise data for obtaining reflection loss and geoacoustic properties. Further, we explore the feasibility of using very short vertical apertures (1–5 m). We begin by describing noise modeling— this is useful to illustrate how beamforming ambient noise can produce reflection loss and also is the basis for the inversion technique for determining geoacoustic properties of the seabed. This noise modeling is appropriate for high frequencies and broad band data since it is built on a ray approach. The next section gives a short description of the beamforming issues that, in some cases, hinders obtaining the ambient noise inversion. Finally, data from the recent ElbaEx experiment [3] is used to demonstrate the inversion technique.

HIGH FREQUENCY AMBIENT NOISE MODELING AND ESTIMATING REFLECTION LOSS

A variety of methods exist for modeling the ocean's acoustic ambient noise field [4]. Probably the most widely used methods are normal modes (Kuperman-Ingenito) or wavenumber integration [5, 6]. These wave solutions are not ideal for high frequency, or broadband calculations since they become too computationally intensive. Since we are considering both broad-band and high-frequency data for inversion these methods are not attractive. Here, a simpler ray approach is used which involves far fewer calculations yet provides (arguably) a better solution than full-wave models [7]. A broad-band of frequencies can be computed at arbitrarily high frequency in a fraction of the time needed for wave calculations and this type of calculation is included in the noise coherence model CANARY [8, 9].

A ray based derivation will be presented here for the noise cross-spectral density function that follows Harrison [7] but simplified by only considering vertically separated

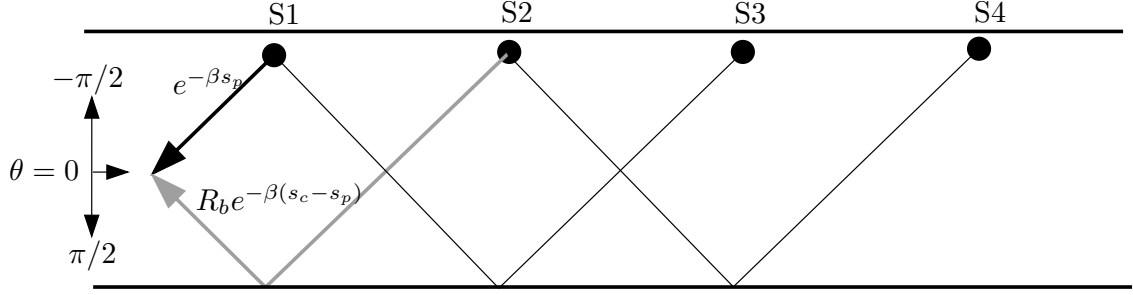


FIGURE 1. The geometry for noise sources near the surface. The sources shown are those that would arrive at a location from equal angles looking toward the surface and towards the seabed. A full cycle distance is indicated by s_c and partial (from S1 to receiver) by s_p and bottom reflection loss by R_b . The coordinate system for up and down looking angles is shown on the left side of the diagram.

hydrophones in an iso-sound speed water column (these assumptions are not required; but making them allows for a more clear derivation to illustrate the method).

The acoustic field at frequency ω can be calculated from ray amplitudes and arrivals at a receiver depth, z_r and range r according to,

$$P(\omega, z_r, r) = \sum_{n=1}^N A_n e^{i\omega D_n}, \quad (1)$$

where A_n are the arrival amplitudes for the n^{th} eigenray and D_n the corresponding delays. The noise cross-spectral density function between two vertically separated hydrophones at depths z_1 and z_2 ($z_2 > z_1$) is,

$$C_\omega(z_1, z_2) = \int_0^{2\pi} \int_0^\infty P(z_1) P^*(z_2) g^2(\theta) r dr d\phi \quad (2)$$

where $g(\theta)$ is a term that allows for the noise sources to have directionality. If the noise sources are dipoles and we assume azimuthal symmetry,

$$C_\omega(z_1, z_2) = 2\pi \int_0^\infty \sum_n |A|^2 e^{ik(z_2-z_1)\sin\theta} \sin^2\theta r dr. \quad (3)$$

In eq. (3), the cross terms of the double sum have been ignored. The final step is to include the amplitude term which for each path is,

$$|A|^2 = \frac{\cos\theta}{r|(dr/d\theta)\sin\theta|} Q P_m \quad (4)$$

where Q and P_m are needed for the volume and boundary losses. The value of these terms are illustrated using Fig. 1 where four noise sources are shown that contribute to a receiver in the water column from the same angles in the upward and downward directions.

The first source has only volume losses to the receiver, $Q = e^{-\beta s_p}$, where β is the volume loss per distance and s_p is the ray partial cycle distance. The losses from the

second source include a longer path and a bottom interaction: $Q = e^{-\beta(s_c - s_p)} R_b$, where s_c is the complete ray cycle distance and R_b is the bottom reflection loss. Each of the next sources also include losses from one or more full cycle distance which results in a geometric series for the compounding losses. That is, $P_m = \prod_{m=1}^m R_b e^{-\beta s_c}$, or, for angles between $-\pi/2$ to 0 (sources S3, S5, S7 ...),

$$Loss_{-\pi/2 \rightarrow 0} = e^{-\beta s_p} \{1 + R_b e^{-\beta s_c} + (R_b e^{-\beta s_c})^2 + \dots\} = e^{-\beta s_p} \frac{1}{1 - R_b e^{-\beta s_c}}. \quad (5)$$

For angles between 0 to $\pi/2$ (sources S2, S4, S6 ...),

$$Loss_{0 \rightarrow \pi/2} = e^{-\beta(s_c - s_p)} R_b \{1 + R_b e^{-\beta s_c} + (R_b e^{-\beta s_c})^2 + \dots\} = e^{-\beta(s_c - s_p)} R_b \frac{1}{1 - R_b e^{-\beta s_c}}. \quad (6)$$

Combining these, the cross-spectral density can be written,

$$C_\omega(z_1, z_2) = 2\pi \int_0^{\pi/2} \frac{1}{1 - R_b e^{-\beta s_c}} \cos\theta \sin\theta \{e^{ik(z_2 - z_1) \sin\theta} + R_b e^{-ik(z_2 - z_1) \sin\theta}\} d\theta, \quad (7)$$

where the small partial cycle distance volume attenuation terms have been suppressed. Note in eq. (7) the rdr term has cancelled and the integration is over angle θ . There are two plane-waves in eq. (7); one traveling from the surface down and one from the seabed up. These differ by exactly the term R_b , the power reflection coefficient. Therefore, if beamforming is ideal and these plane-waves could be extracted and corresponding up and down angles divided, then the reflection loss at each angle would result. Note, that even though several assumption were made (such as dipole sources) these are not important factors in the final result since these terms would cancel out when dividing up and down plane-waves.

Vertically beamforming from short or undersampled arrays

As mentioned, if beamforming is ideal the downward traveling plane-waves can be separated from those traveling upward and taking the ratio exactly produces the power reflection loss of the seabed. If array length and hydrophone spacing are sufficient the beamforming is close enough to ideal and the technique produces a good estimate of reflection loss. In general, we desire to have the seabed properties characterized over a broad-band of frequencies. Collecting the broad-band ambient noise data is not a problem, but beamforming and dividing up and down plane-waves can be. Consider a 32 element array designed for 4 kHz (hydrophone spacing of 0.18 m and length of 5.58 m). In the top two panels in Fig. 2 the beampattern is shown for 4 kHz looking both broadside and endfire. Looking broadside, the beam is narrow, about $\pm 2^\circ$ at 6 dB down, and looking endfire about $\pm 5^\circ$. Either broadside or endfire show sidelobes that are down significantly (around 13 dB). When steering near endfire the up and down beams will be distinguishable when the steer angle is greater than about 2° . Likewise, as the beams move from broadside to endfire the reflection loss curve will be “smudged”, but

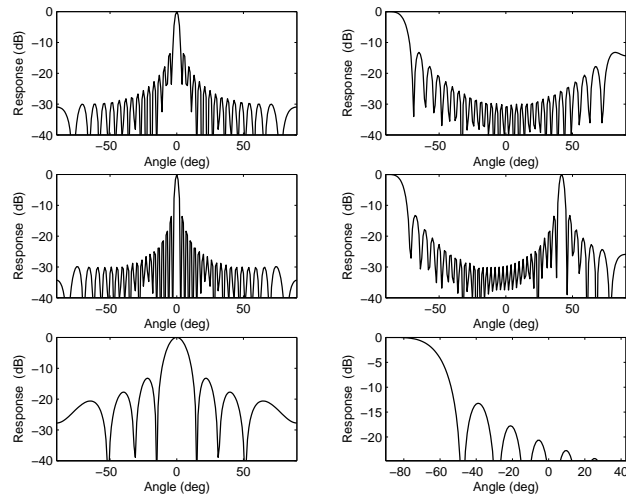


FIGURE 2. Beamformed output for frequencies of 4 kHz (top two panels) 5 kHz (middle) and 1 kHz (bottom). All use an array with 0.18 m hydrophone spacing and length of 5.58 m. Left panels show broadside beamforming and right panels endfire.

only slightly. The smudge is never worse than 10° so, at this frequency, for this array the reflection loss estimate should be good. Now consider beamforming at 5 kHz as shown in the middle panels of Fig. 2. In this case, as we move away from broadside to endfire there is aliasing that forms a beam in the downward direction. This beam will also contribute and these contributions destroy the reflection loss estimate. Next, consider beamforming at 1 kHz shown in the lower panels of Fig. 2. Here, there is no aliasing but the beamwidths are very large, over $\pm 30^\circ$ at endfire. These large beams will cause such a severe smudging that the up/down ratio is no longer a good representation of reflection loss.

GEOACOUSTIC INVERSION OF HIGH FREQUENCY AMBIENT NOISE DATA

ElbaEx 2003

In October 2003, in collaboration with the NATO Undersea Research Centre, a series of experiments took place to the north and south of Elba Island in the Mediterranean Sea. These experiments were designed to study high-frequency acoustic propagation and the performance of underwater acoustic communications. On October 29, 2003, an ambient noise experiment was conducted at the north site near Capraia Island. An array with 32 hydrophones having 0.18 m separation was allowed to drift from an initial position of $42^\circ 55.5'N$, $10^\circ 5.4'E$ while recording ambient noise. The low end of the spectrum was only filtered to prevent interference from mechanical noise at the high end, an anti-aliasing filter cut the data off at around 3.8 kHz. Only data below 3.5 kHz are considered here. The water column sound speed profile was slightly downward refracting with a late

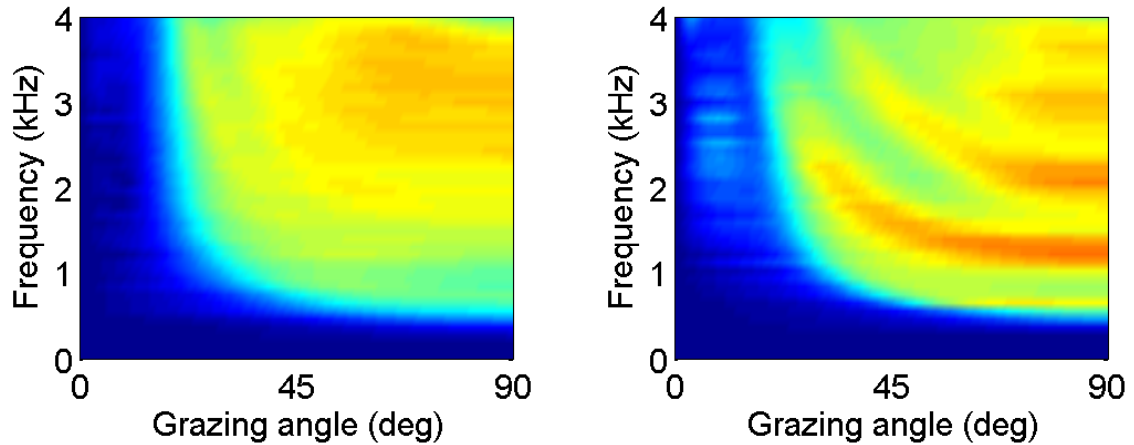


FIGURE 3. Reflection loss inferred from noise measured on a drifting VLA. The left panel shows 4 minutes of data from 11:30 UTC and the right panel 4 minutes from 13:00 UTC processed by beamforming and dividing the upward and downward looking beams. Data are shown on a 0-15 dB color scale.

summer type profile. The ambient noise data were processed to form the cross-spectral density matrix and in the following sections the reflection loss and seabed properties are estimated from about four minutes of data.

In Fig. 3, two examples are shown taking measured ambient noise, followed by forming the cross-spectral density, vertically beamforming and dividing the beams looking toward the surface by those steered towards the seabed. There are two notable differences between the left panel (11:30 UTC) and the right (13:00 UTC): first, there is an interference pattern evident in the right panel that is absent in the left panel. These type of fringe patterns are formed from layers in the seabed and already by observation the left panel can be represented (for these frequencies) as a homogeneous half-space. The second difference is the slightly higher loss near grazing angles in the data shown in the right hand panel. In the next section we use an inversion scheme to determine the seabed properties from these data.

Inverting reflection loss

One of the most attractive features of the up/down, ambient noise inversion is that it isn't really an inversion. It is an extremely simple processing technique to produce the reflection loss curve. In some cases, this reflection loss curve may be all that is required. For propagation modeling, particularly ray based models, this is a sufficient representation of the bottom. However, as we have seen, actual arrays introduce a beampattern that will smudge the reflection loss and this is not always a good representation of the true reflection loss. Also, for angles near horizontal small errors in correcting for diffraction or array tilt (or other experimental errors) can cause slightly offset beams and therefore errors in the reflection loss estimate for these angles. In addition, we seek to invert the

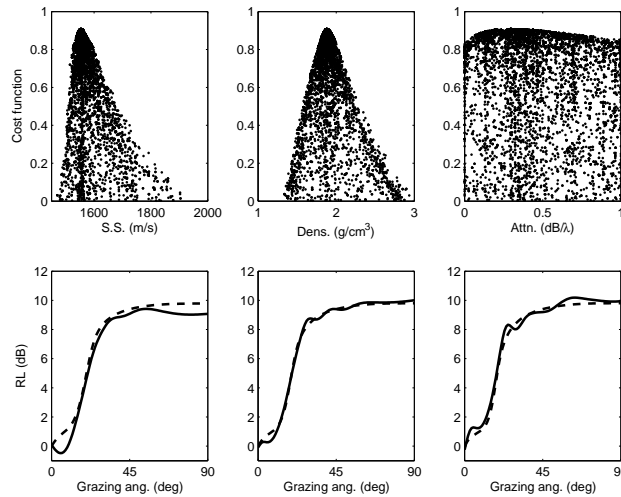


FIGURE 4. Top panels show the cost function output from the genetic algorithm search with the seabed parameterized by sound speed, density and attenuation (x-axes indicate the search bounds). The peaks indicate where the best fit occurs; for the 11:30 UTC data the best fit values are: sound speed: 1553 m/s; density: 1.9 g/cm³; attenuation 0.3 dB/λ. Lower panels show the measured up/down ratio (solid lines) and the best fit modeled up/down ratio. Left panel is 2 kHz, middle is 2.7 kHz and the right panel 3.5 kHz. These are approximations to the reflection loss curves at these frequencies.

inferred reflection loss to produce geoacoustic properties of the seabed. While these are not always needed, the inversion insures the seabed properties have physical meaning consistent over a broad-band of frequencies and can be used to correct the errors and smudging in the estimated reflection loss. In theory, once the correct geoacoustic properties are determined they can be used over all frequencies.

All the effects introduced into the measured data from the environment, such as water column sound speed profile, surface losses, volume attenuation and physical array parameters (length, number of hydrophones) can be included in the formula for noise cross-spectral density (eq. (7)). This, can then be beamformed and the up/down beam ratio taken in exactly the same way as for the measured data. To produce a true reflection loss and geoacoustic properties the beamformed output and/or the up/down beam ratio can be compared with the model results using a variety of environments and a search algorithm to find the best. In our case, we compare the mean square error between measured and calculated quantities and direct the search using a genetic algorithm. A genetic algorithm is useful since the number of geoacoustic properties can be large depending on the number of layers in the seabed. Exhaustive searching for the best fit quickly becomes unwieldy. The number of layers to include in the model can be estimated by transforming the reflection loss into an impulse response using the sub-bottom profiling technique [2]. The data considered here first is from 11:30 UTC where there is no evidence of structure in the reflection loss curves (see Fig. 3) and, therefore, a simple half-space was used to describe the seabed (i.e. a sound speed, density and attenuation constant).

In Fig. 4, the results are shown from the processing in the 2–3.5 kHz band with the 32 elements of the array (5.58 m length). In the lower figure, the solid line represents

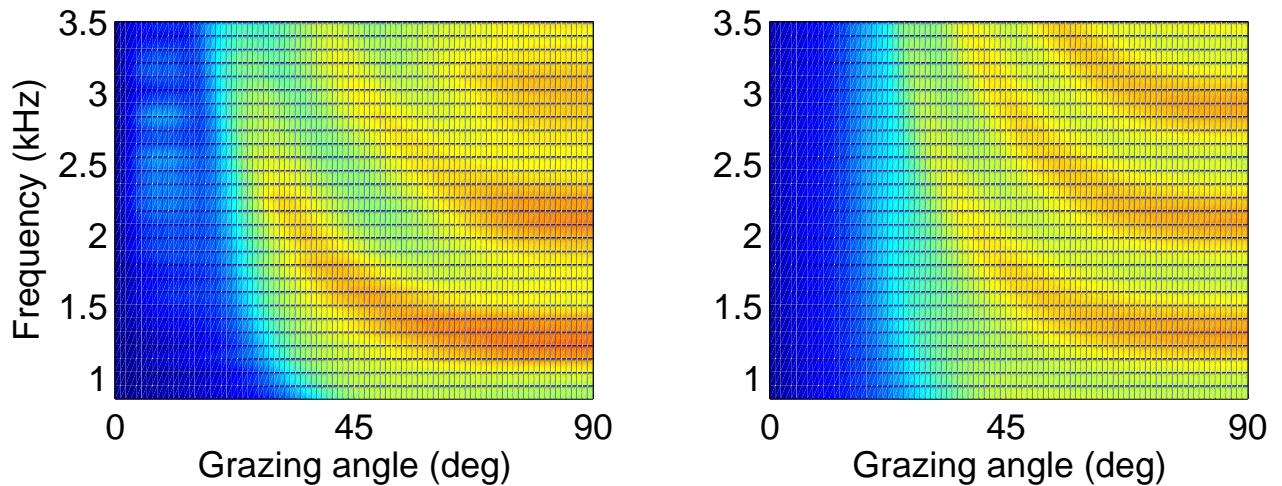


FIGURE 5. Experimental data (left panel) and model (right panel) of the up/down beam ratio. The model has a sediment layer of 0.99 m over a half space. The sediment properties found are: sediment sound speed: 1561 m/s, sediment density: 1.91g/cm^3 , sediment attenuation: $0.6\text{ dB}/\lambda$, half-space sound speed: 1625 m/s, density: 2.1g/cm^3 , attenuation: $0.002\text{ dB}/\lambda$.

the inferred reflection loss at 2, 2.7 and 3.5 kHz determined from taking the ratio of up to downward steered beams. These reflection loss estimates are compared against thousands of possible seabed types that are used to calculate cross-spectral density, beamformed and further processed for the up/down reflection loss estimate. The output values of the cost function for each of the three seabed parameters are plotted against the seabed property value (the x-axes indicate the search bounds for each parameter). The peak indicates the point having best agreement with the data. There are clear indications that the seabed sound speed, density and attenuation are well determined from the data. In the lower panel of Fig. 4, the dashed lines show the output from the model. Note, that the processed measured data has unrealistic values of reflection loss at low angles but realistic values come out of the model. Once the seabed properties are obtained, the “true” reflection loss curves can be generated at any desired frequency without the beamforming “smudging”.

In another example, four minutes of data are taken at about 13:00 UTC and the up/down beam processing is used with the results shown in the right side panel of Fig. 3. In this case the fringe pattern indicates the presence of a layer in the seabed. Therefore, a seabed layer over a half-space was the assumed geoacoustic seabed for inversion and this has 7 parameters (sound speed, density and attenuation in the sediment layer and halfspace and the sediment thickness). The final result shows a sediment layer of 1 m and the model/data inferred reflection loss comparison is shown in Fig. 5. While the sound speed in the sediment layer for the 13:00 UTC data is similar to the previous example at 11:30 UTC, the attenuation constant found at 13:00 is higher. This appears consistent with the measurements for the region at low grazing angles where the bottom loss is greater (comparing low grazing angles in the left and right panels of Fig. 3. In this example data from 1–3.5 kHz were used.

TABLE 1. Seabed properties found through inversion of ambient noise (11:00 UTC) data using different array configuration and geoacoustic parameterization of the seabed.

	Sound speed (m/s)	Density (g/cm ³)	Attenuation (dB/λ)
32 phones-5.54 m	1553	1.9	0.30
8 phones-1.44 m	1546	1.9	0.13
16 phones-5.4 m *	1567	2.0	0.35

* Beamformed output used for model/data comparison

Inverting beamformed data from short or undersampled arrays

In the previous examples, the full array which is 32 hydrophones with 0.18 m spacing (total length of 5.58 m) was used. Here, we consider reducing this in two ways, first, 8 hydrophones are used for about 1.4 m aperture. Then, 16 hydrophones with 0.36 m spacing is considered (5.4 m total length). For the case with 1.4 m and 8 hydrophones the beams become large and the up/down ratio of beams smudges the reflection loss to the point where it no longer reasonably represents the reflection loss. However, using the modeling the smudging is done in exactly the same way and, somewhat surprisingly, the final seabed values are nearly the same as those found using the full array. In the second case, the sparse sampling of hydrophones causes grating lobes that destroy the up/down ratio and the results do not even resemble reflection loss curves. However, in this case, the beamformed output is compared (rather than the up/down ratio) with that from the model (i.e. the final step of forming the up/down ratio is skipped). Even though the beamformed output has grating lobes, the model is the same and again the final seabed values found using the search algorithm are nearly the same as for the other examples. All these results are summarized in Table 1 for the data at 11:00 UTC.

CONCLUSIONS

In this paper we examined the possibility of using ocean ambient noise data in the 1–4 kHz frequency band to determine properties of the seabed. A noise model based on a ray approach was used along with a genetic algorithm search to match measured and simulated data. This approach compensates for the beamforming “smudging” of the reflection loss as well as for artifacts that sometimes occur for low grazing angles. A genetic algorithm was used to direct the search and find the best fit between model and data with the best fit assumed to be a good representation of the seabed. The tests showed well determined seabed properties and a good match between measurements and model. The seabed properties are also sensible based on preliminary assessment of grain sizes (from a grab sample) and impulse response measurements taken at various ranges using a vertical array and a controlled sound projector. Ambient noise in this band of frequencies and possibly even higher frequencies appears to have advantages of reduced array length requirements and also less interference from shipping. With the short arrays

considered here it may be feasible to use this method for surveys either using surface ships or submerged vehicles such as autonomous underwater vehicles (AUV's).

ACKNOWLEDGMENTS

The authors would like to thank the NATO Undersea Research Centre and the staff that participated in the ElbaEx experiments. In particular, Chief Scientists Finn Jensen (1st half) and Mark Stevenson (2nd half), Engineering Coordinator, E. Michelozzi, and Data Acquisition Coordinator, P. Boni. We would also like to thank the Captain and crew of the R/V Alliance. This research was supported by the Office of Naval Research, Ocean Acoustics Program and the NATO Undersea Research Centre.

REFERENCES

1. Harrison, C. H., and Simons, D. G., *J. Acoust. Soc. Am.*, **112**, 1377–1389 (2002).
2. Harrison, C. H., *J. Acoust. Soc. Am.* (to appear) (2004).
3. Jensen, F. B., “Results from the Elba HF-2003 experiment,” in *Proceedings of the High-Frequency Ocean Acoustics Conference*, AIP, 2004.
4. Jensen, F. B., Kuperman, W. A., Porter, M. B., and Schmidt, H., *Computational Ocean Acoustics*, American Institute of Physics, Inc., New York, 1994.
5. Kuperman, W. A., and Ingenito, F., *J. Acoust. Soc. Am.*, **67**, 1988–1996 (1980).
6. Schmidt, H., *OASES users guide and reference manual*, MIT, Dept. of Ocean Engineering (1999).
7. Harrison, C. H., *J. Acoust. Soc. Am.*, **99**, 2055–2066 (1996).
8. Harrison, C. H., *Applied Acoustics*, **51**, 289–315 (1997).
9. Harrison, C. H., Brind, R., and Cowley, A., *J. Comp. Acoust.*, **9**, 327–345 (2001).